ACS Photonics

pubs.acs.org/journal/apchd5

Article

Ultrahigh Angular Selectivity of Disorder-Engineered Metasurfaces

Mohammad Haghtalab,* Michele Tamagnone, Alexander Y. Zhu, Safieddin Safavi-Naeini, and Federico Capasso

Cite This: *ACS Photonics* 2020, 7, 991−1000

Read Online

ACCESS | Metrics & More | Article Recommendations | Supporting Information

ABSTRACT: Metastructures hold promises for the realization of novel optical functions. Common topologies utilized in the form of metasurfaces featuring simple periodicities, however, are not exploiting the full potential such platform can offer. On the other hand, disordered metasurfaces consisting of strongly coupled elements can provide a versatile platform with large degrees of freedom to be exploited in an inverse design process. Here, we investigate a new class of disordered metasurfaces; a disordered network of scattering elements strongly connected through interelement free space coupling and excited guided waves. Such a highly connected network of scatterers exhibits very strong angular sensitivity for the plane waves illuminating the structure at arbitrary angles; a minute deviation in the angle of incidence results in a drastic change in the radiation profile both in near and far-field regions. This peculiar feature is harnessed by engineered disorder implemented through a rigorous near-optimal freeform inverse design algorithm to realize arbitrarily large metasurfaces with unexpected angular single/multifunctionality. Our proposed scheme is extendable to implement novel functions demanded by emerging applications such as LiDARs and highly secure communication systems.

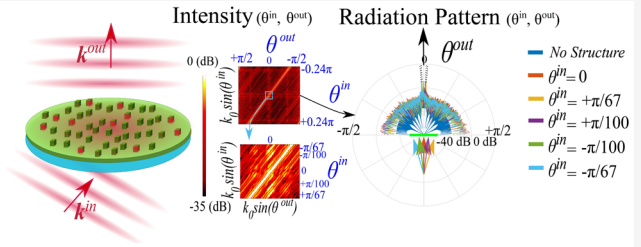

KEYWORDS: *metasurface, engineered disorder, inverse design, guided waves, multifunction, beamforming*

Metasurfaces are the planar realization of metastructures where elements of subwavelength dimensions and separations over flat interfaces can enable unprecedented engineering of light−matter interaction. Not only have they been shown to be an extremely compact alternative to conventional bulky optical devices,[1,2] but also, new functions have been demonstrated[3−6] that are either impossible or very difficult to achieve through traditional approaches. The common types of metasurfaces are based on introducing abrupt changes of optical/electromagnetic properties at an interface utilizing dielectric or metallic nanostructures.[7,8] In the most common technique, the design of each metasurfaces unit cell is carried out separately. This is based on the assumption that the phase, amplitude, and polarization of the incident fields can be independently manipulated within each unit cell; thereby, the wavefront of the incident fields can be controlled at will, leading to the desired behavior in the near- and far-field regions, such as lensing over a desired region in space or collimating or deflecting the incoming optical waves toward a desired angle(s). However, the intercell couplings, also known as mutual coupling in antenna theory,[9] are usually not rigorously taken into account in this approach, and they can cause uncontrollable undesired effects, such as a significant drop in efficiency for high deflection angles. The periodicity inherent in such structures, also, can introduce diffraction orders that further affect the maximum achievable efficiency and reduce the available degrees of freedom to implement novel functions.

Depending on the type of the elements utilized in the proposed structures, namely, resonant or non(weakly)-resonant elements, there are other limitations in terms of the maximum efficiency that can be achieved for various design specifications. These limitations are imposed either due to the undesired intercell couplings throughout the structure or the intrinsic resonant characteristics of the elements within each unit cell. As such, new strategies for designing metasurfaces with higher efficiencies have been proposed.[10,11]

In the new approaches, the strong intercell and intracell couplings are taken into account and exploited to alleviate the fundamental limitations imposed by disordered conventional designs. The inherent large degrees of freedom provided by this new class of metasurfaces are also harnessed to realize novel functions. In a series of studies, employing methods based on topology optimization (TO), freeform metastructures are shown to be promising candidates for the realization of

Received: November 21, 2019
Published: March 24, 2020

https://dx.doi.org/10.1021/acsphotonics.9b01655
ACS Photonics 2020, 7, 991−1000

novel devices like metalens concentrators, multiwavelength focusing, and aberration-corrected metalenses.[10] In other studies, new disordered metastructures are designed to significantly enhance the information capacity through "engineered disorder" in an otherwise low-resolution imaging or low-capacity communication system.[12] Despite all these interesting features, the complexity of the proposed structures prevents a detailed description as to how the physics underlying the wave−matter interaction inside such devices leads to such functionalities. Although the couplings and their collective effects have been the key factors exploited in such designs, there are still open questions regarding the practical and efficient ways to controllably enhance these couplings throughout the structure and how new designs can benefit from this. Furthermore, the challenging experimental implementation, considering all the expected fabrication imperfections, makes the prospective of future use of the suggested designs unclear. Therefore, it is of practical interest to investigate alternative solutions.

Here, we explore a new approach in the design of metasurfaces with features not found in common realizations; this has been enabled through structures that bear the physical properties of disordered systems giving rise to features such as localization and inherent large degrees of freedom and, at the same time, being compatible with current fabrication tools constraints and state-of-the-art techniques. We explore disordered metasurfaces realized by scattering elements which are strongly coupled through both free space and excited guided waves within the structure. As a result of the strong coupling existing between the elements, the proposed structures do not exhibit the strong optical memory effect[13] in the scattered fields due to the incident plane waves illuminating them at various angles. We demonstrate that engineering disorder in the presence of strong coupling can lead to the realization of high angular resolution functions in such devices, i.e. highly angular sensitive structures that are designed to produce desired radiation profiles just for a particular preset incident plane waves. Very small deviation in the angle of incidence leads to a significant change in the radiation profile. Disorder-induced localization of guided waves within the metasurface plays the paramount role in achieving such characteristics. In a general sense, disorder restricts the spatial extent of the excited guided waves within the structure. However, at the same time, it can be engineered to manipulate the induced fields inside the scattering elements, which are the actual launchers of the guided waves and main contributors to the scattered fields. In other words, engineered disorder can enhance and/or attenuate the localization of guided waves in such a way that the required field distribution is generated inside the metasurface elements leading to the desired far-field radiation. The engineered configuration enhances the propagation of the excited guided waves by certain elements while it prevents the excitation or long-range propagation of excited guided waves by most of the elements. This feature is of critical importance to achieve the desired behavior; that is, engineered disorder allows controlling the excitation and coupling of guided waves to the free space radiating modes. It is worth mentioning the fact that "intrinsic disorder" provides interesting properties explored in various applications in photonics.[14,15] On the other hand, the area of "engineered disorder" has opened new avenues for engineering the wave matter interactions in emerging applications.[12,16] Similar to the behavior of dynamical systems that are highly sensitive to the initial conditions, the radiation of the designed metasurfaces is eminently sensitive to the incident plane waves. Unless the designed metasurfaces are illuminated by the predetermined incident waves, which set the initial conditions in the electrodynamic problem, they will strongly attenuate the propagation of all the excited guided waves, which are the important factors contributing to the far-field radiation in such devices. Such high sensitivity can be exploited to realize novel functions. In addition, with more realizable angular functions within a given small range of incident angles, high angular sensitive metastructures can enhance the conventional metadevices in terms of the number of functions which can be realized through them. This opens up a new prospect for achieving ultracapacity metadevices.[17]

CONCEPT

Pioneered by Philip Anderson,[18] the study of localization due to disorder has become of great technological and theoretical importance. Inspired by this phenomenon, we take on a new approach to the problem of engineering the light−matter interaction based on exploiting the disorder-induced localization of guided waves in a metasurface platform. We consider a multilayer structure consisting of a disordered arrangement of subwavelength scattering elements on a top layer, and a mid layer dielectric slab located above a substrate (Figure 1). Under optical illumination, the scattering elements are strongly coupled through multiple scattered waves propagating in free space (short-range coupling) and through the guided waves inside the dielectric slab (long-range coupling). The strong coupling between the elements, enabled by the guided waves, provides more degrees of freedom in manipulating the induced fields inside the elements, which are highly dependent on the initial conditions set by the incident external fields. In the absence of coupling or when the elements are weakly coupled, however, the fields induced inside elements are weakly dependent on the surrounding elements. Consequently, the radiation due to different illuminating conditions, such as different angular directions, becomes highly correlated, affecting the number of functions that can be realized through such platforms. On the other hand, the waves scattered from highly coupled elements can strongly interfere and lead to the localization effects while providing larger degrees of freedom in the design space.

There are three effects that stimulate the localization. First, the interplay between the excited guided waves and the disordered arrangement of scattering elements leads to the localization of the guided waves inside the metasurface. The localization of guided waves stems from their random interference as they propagate and interact with the optical elements. The guided waves propagating inside the randomly corrugated dielectric slab experience discontinuities in phase and amplitude as they pass by each scattering element on top. Due to these interactions, guided waves are partially reflected in the opposite direction and partially transmitted in the original direction. For large enough disorder, the multiple scattered guided waves interfere destructively and, consequently, can become spatially localized. In a similar situation, as shown in ref 19, the transmission of plane waves through random stack of dielectric slabs is strongly reduced due to the disorder. The second effect stimulating the localization of guided waves is the radiation loss as they travel inside the corrugated dielectric slab and get coupled to the radiating modes of free space outside the dielectric slab. The free space

https://dx.doi.org/10.1021/acsphotonics.9b01655
ACS Photonics 2020, 7, 991−1000

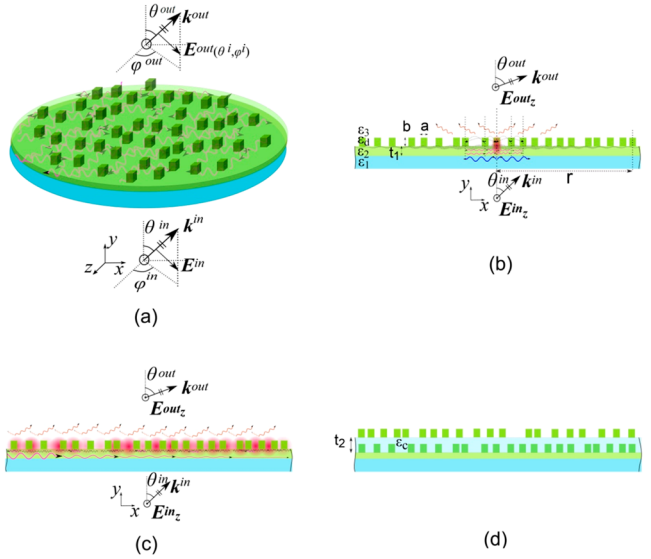

Figure 1. Multilayered disordered metasurfaces. (a) A general schematic. Scattering elements, located on top of a dielectric slab, are strongly coupled through long-range guided waves excited inside the multilayer medium as well as free space short-range coupling between elements. (b, c) The focus in the current work is the two-dimensional version of the structure in (a) consisting of scattering lines located on top of a waveguide. Three mechanisms trigger the localization of excited guided waves. The first is the disorder causing destructive interference of guided waves which causes their localization. The second is the radiation loss due to the presence of scattering elements on top. The third is the free space interelement coupling of disordered elements. (c) For a given plane wave incident on the sample at θ^{in}, the disorder engineered metasurface localizes the far-field radiation at a preset angular direction denoted by θ^{out}. Thanks to high angular sensitivity of such designs, small changes in the incident angle, θ^{in}, result in totally different far-field radiation pattern. (d) To enhance the conversion efficiency of the incident fields into the guided waves, while preserving the angular sensitivity of structure, a multilayer scheme can be used.

short-range coupling between the scattering elements, additionally, is the third effect causing the localization. This effect is mathematically explained through symmetrical random band matrices modeling the coupling between the randomly configured scattering elements. As shown in ref 20, as a result of introducing randomness to such matrices, the localization length of the eigenvectors is significantly reduced. In a similar manner, introducing randomness to the locations of highly coupled elements results in significant reduction of the localization length in the eigenvectors. In the Supporting Information (S1 and S2), we present statistical analyses demonstrating how disorder and radiation loss trigger the localization of induced fields inside the elements and the excited guided waves.

It is essential to recognize the two factors contributing to the total radiation from such metasurfaces. The light incident on the metasurface interacts with the scattering elements which impart phase and amplitude modifications to the incident fields. The total scattering fields is the sum of the light that is directly scattered by the elements and the multiple scattered fields, where light scattered by one element is scattered by another one and so on. These scattering fields get partially coupled to the radiating free space modes contributing, as the first component, to the total radiated fields. Most metasurfaces, metalenses, and polarization meta-optics[2−5,7,8] are local, in the sense that they operate based on engineering the first radiating component, which strongly depends on the local modification of the wavefront by the meta-elements neglecting mutual coupling effects. Due to their local nature, these metasurfaces exhibit weak dependence with respect to the incident light angle.[21,22] However, this is not the case for the metasurfaces of our interest in this work. The scattering fields from the elements excite guided modes inside the structures. These modes can interact a second time with the metasurface elements, creating a second component of the radiated field. Due to this effect, these metasurfaces can exhibit strong dependence with respect to the incident light angle.

Recently, it has been shown that guided waves effects can be harnessed to enhance the circular dichroism in nanostructures with chiro-optical activity properties.[23] In another work, the guided mode resonances play a pivotal role in realizing multiwavelength functions by providing larger phase coverage and further decoupling of realized phases at different optical wavelengths.[24] The metasurfaces we investigate in this work strongly rely on the guided waves contribution to the far-field radiation. Due to the typically strong and longer-range coupling, the light interaction with such structures is strongly affected by any small change in the angle of incidence which set the primary phase and amplitude of launched guided waves within the metasurface. Engineering the disordered arrangement of ultra subwavelength scattering elements make the radiation contributed by guided waves more pronounced where, along with the favorable localization effects, the guided mode resonances are taken advantage of to amplify the excited guided waves which is essential for highly efficient realization of desired functions. The interaction between this second radiating component with that of scattering elements without the guided wave effects results in rich scattering features of such structures. Our goal is to control this process by manipulating the excitation, propagation, and the coupling of guided waves to the far-field radiation. Although we employ scattering elements to generate and couple the guided waves into propagating modes, engineering their arrangement, while exploiting the disorder, alleviates the unavoidable undesired scattering effects they introduce to the far-field radiation.

By engineering the disorder, the localization lengths, the phases/amplitudes of excited guided waves, and their coupling to the free space propagating modes can be tailored in such a way that intended functions are achieved by creating the desired near and/or far fields distributions for a given set of illuminating plane wave(s). Illuminating the disorder engineered structures with any other arbitrary set of incident fields leads to the excitation of highly localized guided waves within the structure. Subsequently, the low conversion efficiency of guided waves into the far-field radiation results in low-intensity, close to uniformly distributed noise-like far-field scattered fields mainly due to the direct scattering effects of disordered scattering elements. This high angular selectivity feature allows the incorporation of a larger number of functions each defined for an incident plane wave with a specific angular direction chosen at design time. In the Supporting Information (S3), we provide more detailed explanations on the role of localization in engineering the radiation from disorder engineered metasurfaces.

The number of functions is limited by a few physical parameters including the effective aperture size of the metasurface, determined by the localization length of guided waves, and the conversion efficiency of the incident fields into

https://dx.doi.org/10.1021/acsphotonics.9b01655
ACS Photonics 2020, 7, 991−1000

the guided waves and from guided waves into the desired radiating modes of the free space. As the effective area of the metasurface is increased, narrower diffracted beams can be achieved in the far-field, and thus, the angular resolution or selectivity is enhanced. One of the main roles of scattering elements is to enhance the conversion efficiencies. Nonetheless, they adversely affect the localization length of guided waves. As the level of disorder goes beyond a specific threshold, for example, when the number of scattering elements exceeds a near optimal value, the localization length of guided waves starts to drop and, consequently, the effective radiating aperture and angular sensitivity are reduced. Excessive numbers of scatterers aggravate the unavoidable stray diffractions and impose more radiation loss on the guided waves than they enhance their localization length to improve the angular sensitivity or selectivity. Consequently, the maximum number of functions which can be realized through a given metasurface is reduced. From a different perspective, the light interaction with a structure composed of extremely high density of subwavelength scatterers can be approximated by the effective medium theory meaning that the large degrees of freedom that scatterers could offer in an optimal disorder engineered structure no longer exists when metastructures are overpopulated by scattering elements.

In the next section, we present the design procedure for disorder engineered metasurfaces with high angular sensitivity as explained above. The concept is used to design novel functions such as high angular selectivity, far field angular concentrator, angular negative refraction metasurfaces and ultra selective angular multifunctionality.

DESIGN

We employ a full vectorial electromagnetic approach based on the method of moments (MoM),[25] along with the Complex images Green's function technique[6,26,27] to solve the forward problem in a fast and highly accurate manner. The forward problem is to compute the scattered fields when a given structure is illuminated by a known incident field. A well-known advantage of such technique is that it can accurately and efficiently model the wave interactions with objects through analytical and closed form formulations using the Green's functions of the multilayered background medium. Accurately satisfied boundary conditions through Green's functions alleviate the corresponding numerical errors in other numerical approaches. Employing the Complex images technique, in addition, facilitates the numerical evaluations of the Green's functions required to compute the elements of the matrices in the MoM formulation.

Employing the developed fast forward solver, we use a recently developed algorithm which we call near optimal freeform inverse design (NOFID) approach previously used to design disordered multilayer metalenses.[12] Only recently, approaches based on TO have been employed to optimize metalenses with large degrees of freedom and versatile functions.[11,12] It is important to note that the optimization problem defined for such structures is not convex which typically means that there are several different local minima (maxima), or nonunique solutions.[28] The reported TO approaches are based on the method of gradient descent where initial solutions are iteratively optimized to obtain a local minimum (maximum). On the other hand, due to the large number of variables, most global optimization methods cannot handle this type of problem efficiently. We apply a new approach outlined in ref 12, which is a stochastic-based optimization technique capable of searching for the global solutions based on defined constraints and design parameters. Our proposed approach is based on controlled sets of iterative perturbations of solutions in the solution space. Starting from an initial state (solution), the primary solution undergoes probabilistic changes through an iterative approach. Being controlled by different parameters, this process ultimately leads to an optimized structure in terms of satisfying the defined cost function(s). The evolution of the metasurfaces during each design step strongly depends on the previous (initial) configurations, which are highly randomized. Therefore, due to this probabilistic nature of the optimization algorithm, the algorithm may converge to various solutions for different runs, all satisfying the same design criteria. A similar behavior is observed and studied for topology optimized metasurfaces.[29]

Employing the proposed algorithm (NOFID), we maximize the cost function(s) defined in the optimization process. The optimization is described by the maximin formulation[30] expressed in terms of the Fourier transform of the radiated fields, $\{\mathbf{E}(\mathbf{r})\}$, for a given set of incident fields, $\{\mathbf{E}_{\mathbf{inc}}(\mathbf{r})\}$, which are proportional to the far-field radiation patterns. The maximin formulation, applied to a set of defined functions, can be described as optimizing (maximizing in this work) the worst-case outcome which is the function with the minimum output among others:

$$\underset{\{(x_s, y_s)\}}{\text{maximin}}\{|FFT\{\mathbf{E}(\mathbf{r};\ \{(x_s, y_s)\}),\ \theta_n\}|^2 \colon n = 1, 2, ..., N\} \tag{1}$$

where

$$\mathbf{E}(\mathbf{r};\ \{(x_s, y_s)\}) = \int_{\text{sourceregion}} \mathbf{G}(\mathbf{r}, \mathbf{r}').\ \mathbf{J}(\mathbf{r}')\mathrm{d}\mathbf{r}' + \mathbf{E}_{\text{inc}}(\mathbf{r}) \tag{2}$$

$\mathbf{G}(\mathbf{r},\mathbf{r}')$ is the Green's function associated with the current source, $\mathbf{J}(\mathbf{r}')$, located at $\mathbf{r}'$. Finding the optimum locations for the scattering elements, $\{(x_s, y_s)\}$, is the main objective in the process of optimizing the cost function. Our primary goal is to have the preset incident plane wave(s) deflected toward the angle(s) set by $\{\theta_1, \theta_2, ..., \theta_N\}$, where each member indicates a preset particular angular direction. Using the maximin formulation described in eq 1, the power efficiency and the angular selectivity of the metasurface is modified for all the preset angular directions by adding new scattering elements at suitable locations to the current design set by $\{(x_s, y_s)\}$. The power efficiency is defined as the ratio of the power deflected toward the desired angular direction, θ_n, to the input power of the incident fields, and the angular selectivity as the ratio of the radiated power in the desired angular direction, θ_n, to the maximum radiated power in all other undesired directions. The Green's function, denoted by $\mathbf{G}(\mathbf{r}, \mathbf{r}')$, describes the radiated scattered electric fields, $\mathbf{E}_{\text{scattered}}(\mathbf{r})$, at any arbitrary point in space, called the observation point $(\mathbf{r})$, due to the dipole sources located at $\mathbf{r}'$ radiating in the multilayered background medium with electrical permittivity described by $\epsilon_{\text{bg}}(\mathbf{r}')$. The effective volumetric currents flowing inside the scattering elements can be modeled as $\mathbf{J}(\mathbf{r}') = j\omega(\epsilon(\mathbf{r}') - \epsilon_{\text{bg}}(\mathbf{r}'))\mathbf{E}(\mathbf{r}')$, which are proportional to the total electric fields, $\mathbf{E}(\mathbf{r}')$, induced inside the scattering elements and are responsible for generating the scattered fields, $\mathbf{E}_{\text{scatteted}}(\mathbf{r}')$, at a given frequency ω. The total electric field, $\mathbf{E}(\mathbf{r}')$, can be expressed in terms of the summation of the incident and scattered electric field as $\mathbf{E}(\mathbf{r}') = \mathbf{E}_{\text{inc}}(\mathbf{r}') + \mathbf{E}_{\text{scatteted}}(\mathbf{r}')$. Expanding the unknown current densities, $\mathbf{J}(\mathbf{r}') \propto \mathbf{E}(\mathbf{r}')$, or the total electric

https://dx.doi.org/10.1021/acsphotonics.9b01655
ACS Photonics 2020, 7, 991−1000

fields inside the scattering elements in terms of the pulse basis functions as $\mathbf{E}(\mathbf{r}') = \sum_{m=1}^{M}\alpha_m P_m(\mathbf{r}')$ and applying the point matching technique we arrive at M equations for the M unknowns, α_ms, as $\alpha_k = E_{inc}(r_k) + \sum_{m=1}^{M}\alpha_k Z'_{km}$, where k = 1, 2, ..., M and $Z'_{km} = \int_{P_m}\mathbf{G}(\mathbf{r_k}, \mathbf{r}'_m)\cdot\mathbf{J}(\mathbf{r}'_m)d\mathbf{r}'$. Writing these equations in a matrix form, we obtain $[\mathbf{E}_{inc}] = [Z][\alpha]$, where $[Z] = [[\mathbf{I}] - Z']$ describes the interelement couplings between all scattering elements and $[\mathbf{E}_{inc}]$ and $[\alpha]$ give the incident and total electric fields, respectively, inside the scattering elements. One can solve this matrix equation for the unknowns (total electric fields $[\mathbf{E}]$) and obtain the electric fields over any specific plane above the structure. Taking the Fourier transform of the calculated fields provides the radiation in the far-field region.

We aim at realizing metasurfaces with high angular resolution functionalities in the far-field region. As the first example, we consider highly sensitive angular selective metasurfaces; that is, the metasurface only strongly interacts with the plane wave(s), hitting the structure at a specific particular angle(s) to create the desired output(s) in the far-field. More specifically, we design metasurfaces that only upon interaction with a preset plane wave deflect/localize the incoming waves toward/at an arbitrary direction (in the far-field) set in the design procedure. In the next step, we demonstrate the efficacy of such structures to realize high angular sensitivity functions. Preset plane waves propagating at slightly different angles lead to totally different radiation profiles upon interactions with the designed metasurfaces.

RESULTS

We consider a multilayer structure, as shown in Figure 1. An optical TE illumination (with electric field polarized along z-axis) with a wavelength of 650 nm is assumed. The structure consists of identical TiO_2 elements with rectangular cross sections with dimensions of a and b located on top of a dielectric slab (TiO_2) deposited on a glass substrate (ε_1 = 2.12, ε_2, ε_d = 5.48, and ε_3 = 1 at λ = 650 nm). The midlayer serves as a single mode dielectric slab waveguide with a thickness of t_1 = 65 nm. We apply the freeform inverse design approach outlined in ref 12 to design the configuration of scattering TiO_2 lines on the top layer. Under optical illumination, each of these elements excites guided waves propagating in opposite directions that interfere with each other and get coupled to the free space radiating modes. The design algorithm modifies the structure by adding one scattering element at a time at a location which is found through iterative statistical evaluations of cost function(s). Considering the minimum distance constraint between scatterers, which is set to be 50 nm, the algorithm keeps adding new elements at suitable locations until no additional scattering element can further improve the cost function(s) or the desired function is achieved.

We start by designing structures that only strongly interact with plane waves incident on them at one particular angle. Upon interaction with such group of incident fields, the structure modifies the phase/amplitude of the incident field to generate the desired field distributions in the far field region. We choose to localize the far-field radiation around one specific angular direction only for a preset incident fields. The output angular characteristic is described by three quantities measured over the far-field at a given targeted θ^{out}; namely, the half power beam width (HPBW), the angular persistency, denoted by $\delta\theta^{in}$, defined by the angular range of incident fields (centered at targeted θ^{in}) with which the structure interacts significantly leading to a high intensity field at targeted θ^{out} over the far-field region, and the angular quality factor defined through:

$$Q_{ang}(\theta_{incident} = \theta^{in}) = 1/\Delta\theta^{in} \quad (3)$$

where $\Delta\theta^{in}$ is the angular range centered at the targeted incident angle, θ^{in}, within which the radiated power in the corresponding diffraction order is greater than half of that at targeted θ^{in}. Angular quality factor is an indicative parameter describing the angular sensitivity of a structure (Figure 2). As the localization length of guided waves increases, the angular sensitivity or quality factor is enhanced.

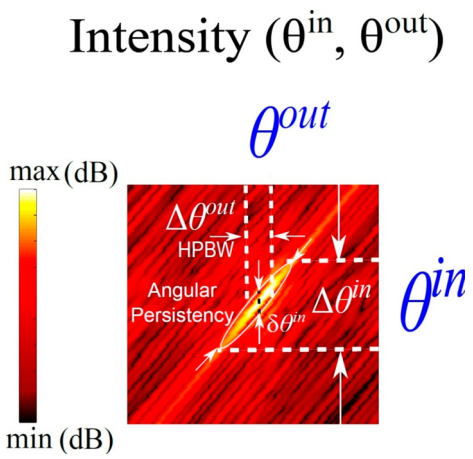

Figure 2. Output angular characteristics in the far field over the targeted angular direction of θ^{out} due to plane waves incident on the designed structures, described by the half power beam width (HPBW), the angular quality factor, Q_{ang}, being proportional to the inverse of $\Delta\theta^{in}$ and angular persistency $\delta\theta^{in}$ shown in black dotted line.

As the first example, we consider one layer of scattering elements with a = 50 nm and b = 50 nm distributed over the range $-62\ \mu m < x < +62\ \mu m$. The structure response to the incident fields, which is sensitive to the angular direction of the plane waves incident on them, is designed to have strong angular effects due to the optical illuminations at close to normal angle ($\theta^{in} = 0$). In other words, only for the normally incident plane waves, the structure is designed to localize the fields, in the far-field region, around a specific angle. Choosing the localization angle as $\theta^{out} = -0.122\pi$, we can achieve a power efficiency of around 9%, which is defined as the ratio of the radiated power toward the desired angle in the far-field to the total power of the incident field in the absence of scattering elements. The geometry is shown in Figure 3a. Also shown are the intensity and radiation patterns, which are normalized with respect to the intensity of the radiated field at $\theta^{out} = -0.122\pi$ when $\theta^{in} = 0$. A half power beam width (HPBW) and angular persistency ($\delta\theta^{in}$) of about 0.002π are achieved. The angular quality factor (Q_{ang}) is around 32.26. As shown, changing the incident angle by a very small amount ($\pm\pi/50$), results in significant changes in the radiation pattern and a drop of around 90% in the power localized around the specified angle ($\theta^{out} = -0.122\pi$). The designed structure is almost transparent to the incident plane waves propagating in all other angular directions except the ones hitting the structure at $\theta^{in} = 0$. In other words, the incident fields propagating at $\theta^{in} \neq 0$ are

https://dx.doi.org/10.1021/acsphotonics.9b01655
ACS Photonics 2020, 7, 991−1000

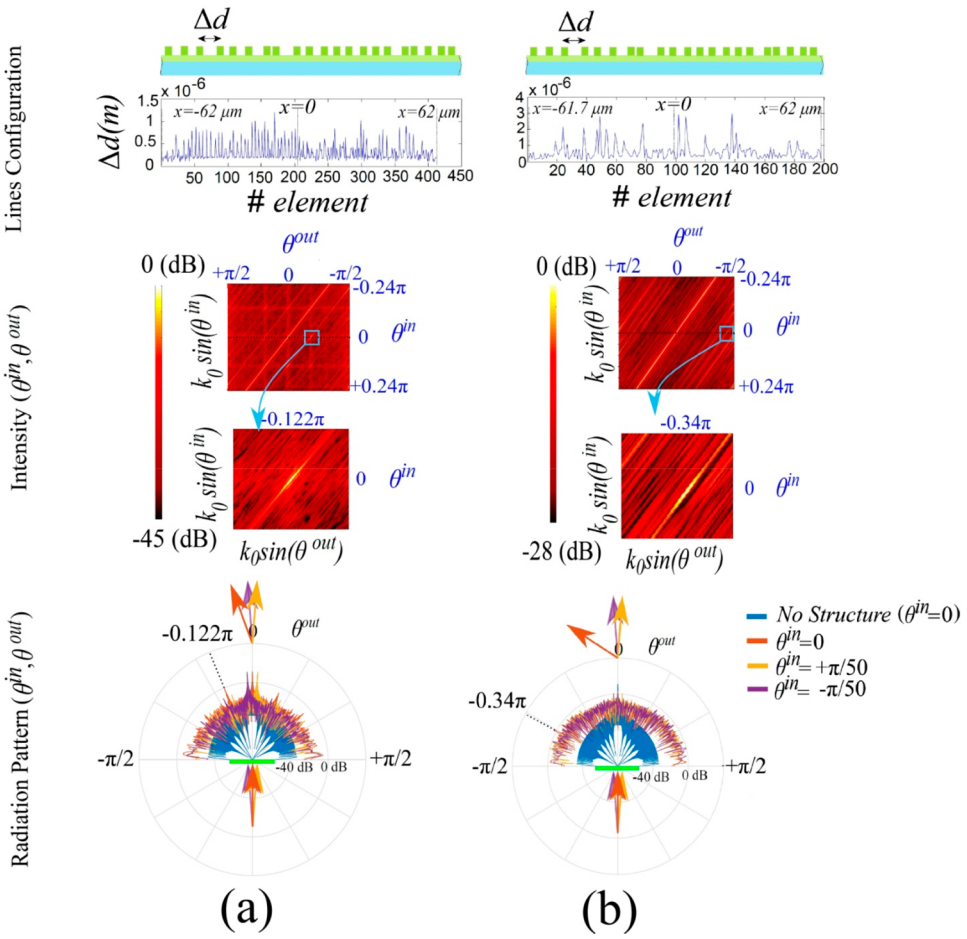

Figure 3. Disorder engineered highly sensitive angular selective metasurfaces. (a) A single layer design with scattering elements (lines) with cross sections of $a = b = 50$ nm partially localizes the normally incident plane waves at $\theta^{out} = -0.122\ \pi$ in the far-field. The achieved power efficiency is around 9%. The angular quality factor, HPBW, and angular persistency ($\delta\theta^{in}$) are 32.26, 0.002π, and 0.002π, respectively. The radiation patterns are normalized with respect to the localized power at $\theta^{out} = -0.122\pi$ for $\theta^{in} = 0$ and correspond to the black dotted lines in the intensity plots. (b) A single layer design with scattering elements (lines) with cross sections of $a = 100$ nm and $b = 300$ nm. Stronger scattering elements enhance the power efficiency from around 9% in (a) to above 15%. To maintain the angular sensitivity of (a), a larger angle ($\theta^{out} = -0.34\pi$) has to be chosen. Larger distances between the elements lead to higher number of diffraction orders appearing in the far-field. In (a) and (b), small changes in the incident angle ($\pm\pi/50$) result in significant change in the radiation patterns with a drop of about 90% and 70% in the power radiated around localization angles: $\theta^{out} = -0.122\pi$ in (a) and $\theta^{out} = -0.34\pi$ in (b), respectively. For incident angles $\theta^{in} \neq 0$, less than 1% of incident power is scattered in other directions ($\theta^{out} \neq \theta^{in}$).

much less scattered in all angular directions ($\theta^{out} \neq \theta^{in}$) except the original direction of the incident fields; on average, less than 1% of the input power is observed to be scattered from the structures. Complying with the reciprocity principle, the structure also interacts with the incoming waves in the same direction as the one generated in the transmitting mode. It is important to highlight the aforementioned fact that for the same design criteria we may end up with a different configuration, in terms of the elements locations, each time the optimization process is repeated. In the Supporting Information (S5), we study this feature for the same design criteria as the one of Figure 3a.

Similar structures to that shown in Figure 3a with the same functionality can be realized. Increasing the size of scattering elements is one strategy to boost the power efficiency in new structures. However, larger radiation loss due to larger scattering elements may adversely affect the localization length of guided waves. To compensate for this effect, the optimizer finds solutions with fewer number of scattering elements within a given area. As a result, the average distance between the elements increases and stray diffraction orders appear in the far-field. Figure 3b shows one realization for larger elements with cross sections of $a = 100$ nm, $b = 300$ nm. Despite the improvements in the efficiency (above 15%), stronger radiations from the large scattering elements reduce the angular sensitivity, especially for close to normal output angles ($\theta^{out} \sim 0$), which is due to the dominating effect of direct contribution of the larger scattering elements to the far-field radiation. To maintain the angular sensitivity in such structures with larger scattering elements, larger deflecting angles can be targeted ($\theta^{out} = -0.34\ \pi$ in this case). Higher conversion efficiency of guided waves into the far-field radiation for larger deflecting angles leads to more pronounced angular sensitivity. The achieved angular sensitivity ($Q_{ang} = 25$) is slightly lower than the previous structure with smaller scattering elements. The HPBW and $\delta\theta^{in}$ (angular persistency) remain unaffected. The intensity and radiation patterns are normalized with respect to the intensity of the radiated field at ($\theta^{out} = -0.122\pi$, $\theta^{in} = 0$) for the designed structure of Figure 3a.

https://dx.doi.org/10.1021/acsphotonics.9b01655
ACS Photonics 2020, 7, 991−1000

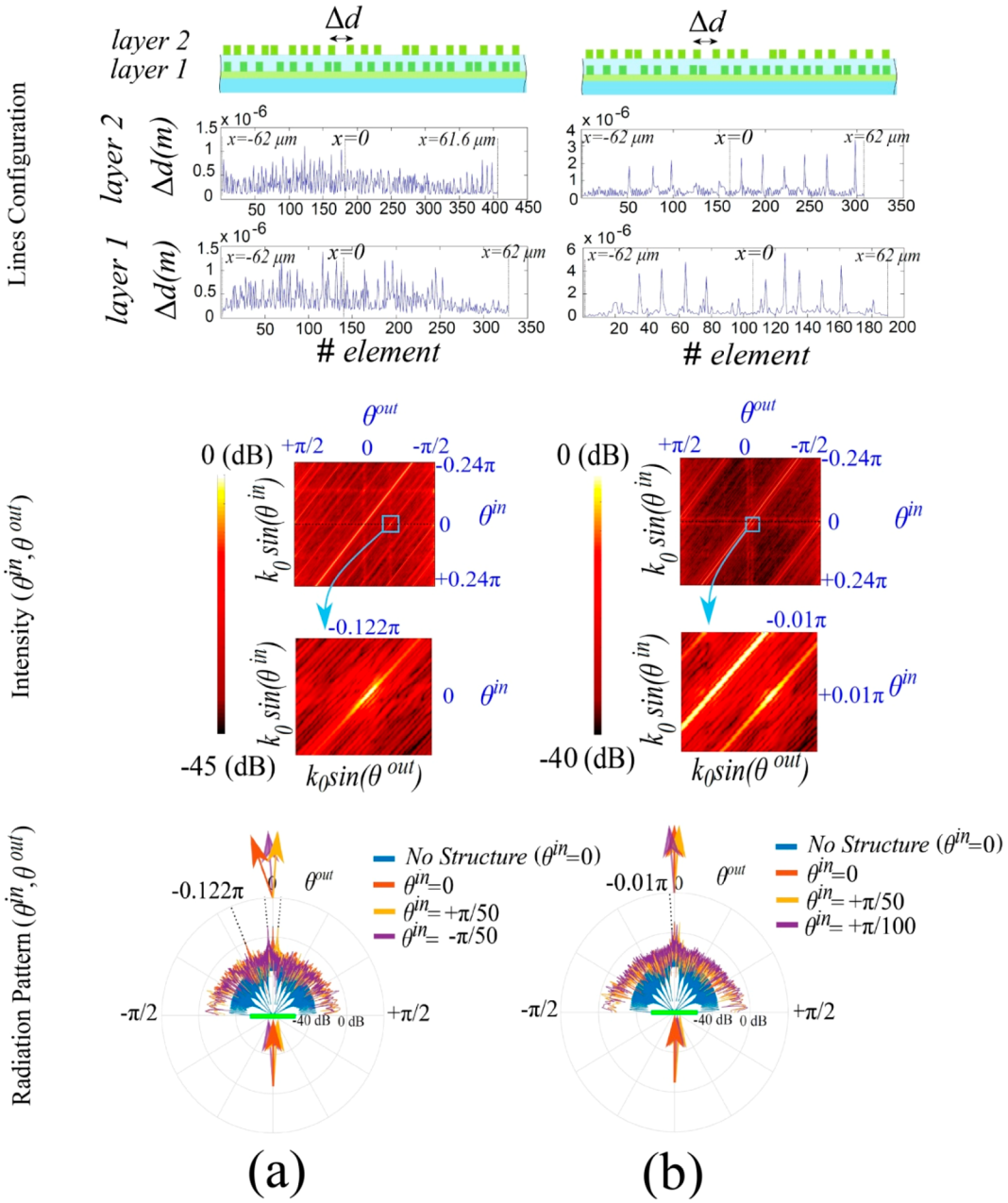

Figure 4. Disorder engineered highly sensitive angular selective metastructures. (a) A two layer design with scattering elements (lines) with cross sections of $a = b = 50$ nm and a distance of 150 nm between two layers, partially localizes the normally incident plane waves at $\theta^{out} = -0.122\pi$ in the far-field. Using two layer structures, an efficiency of above 30% and angular quality factor of 41.6 is achieved. (b) A similar design to (a) that localizes the incident plane waves with $\theta^{in} = +0.01\pi$ at $\theta^{out} = -0.01\pi$. The higher angular quality factor of 77 is attributed to longer localization length of the excited guided waves. Changing the incident angles in both (a) and (b) leads to significant changes in the radiation patterns. A drop of more than 95% in the radiated power around the localization angles is observed.

To improve the power efficiency without sacrificing the angular sensitivity for a wide range of incident angles, we need to enhance the conversion efficiency of the incident fields into the guided waves without imposing excessive radiation loss to the guided waves. A multilayer approach can provide a solution to this problem. Figure 4a demonstrates a two-layer metasurface (t_2 = 150 nm, $\varepsilon_c \approx 1$) realizing the same function as that shown in Figure 3a with improved efficiency (above 30%) and angular sensitivity (Q_{ang} of 41.6). Figure 4b demonstrates a negative refraction structure designed to localize the incident plane waves (only for $\theta^{in} = 0.01\pi$) at far-field angular direction $\theta^{out} = -0.01\pi$, with $Q_{ang} = 77$. As shown, the two-layer scheme allows us to enhance the efficiency while improving the angular sensitivity and not adversely affecting the HPBW or $\delta\theta^{in}$. The intensity and radiation patterns are normalized with respect to the intensity of the radiated field at ($\theta^{out} = -0.122\pi$, $\theta^{in} = 0$) for the designed structure of Figure 3a.

One important feature of disordered structures is that their intended responses, that is, their far-field angular characteristics, are tolerant of the errors associated with the locations of scattering elements. For example, upon applying random errors (up to ±50 nm) to the locations of scattering elements in the structure shown in Figure 3b, a reduction of maximum 30% in the efficiency is observed (down to around 10%), while the

https://dx.doi.org/10.1021/acsphotonics.9b01655
ACS Photonics 2020, 7, 991−1000

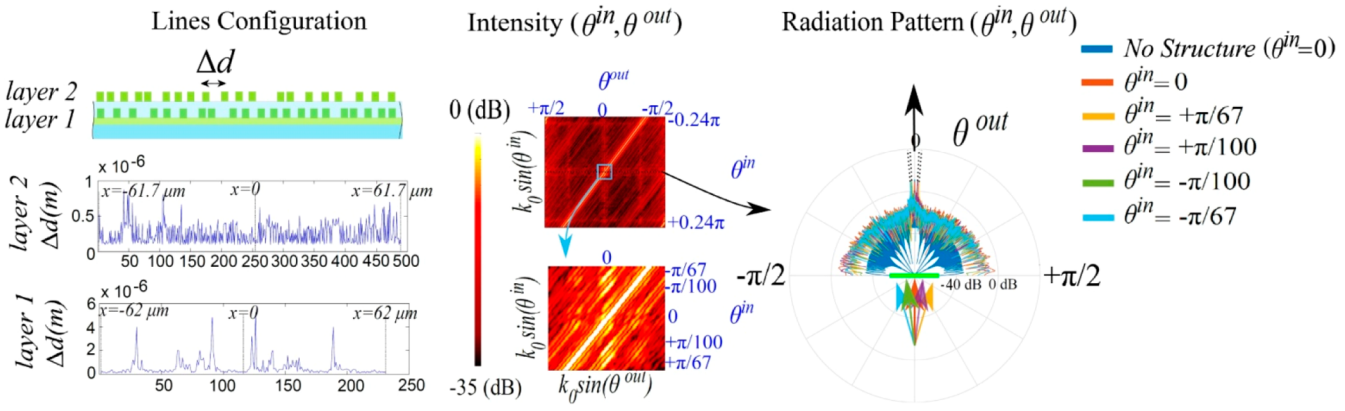

Figure 5. A far-field concentrator is realized using a disorder engineered metastructure. The geometrical size of lines and distance between the layers are the same as those shown in Figure 4. For the preset incident angles, the structure localizes the incident power at $\theta^{out} = 0$ in the far-field. Like previous designs, high angular sensitivity leads to significant changes in the far-field radiation patterns upon changing the incident angles. However, higher angular persistency can be achieved which is a desired effect for such applications. Higher quality factor is obtained. Other angular characteristics are similar to those of Figure 3a.

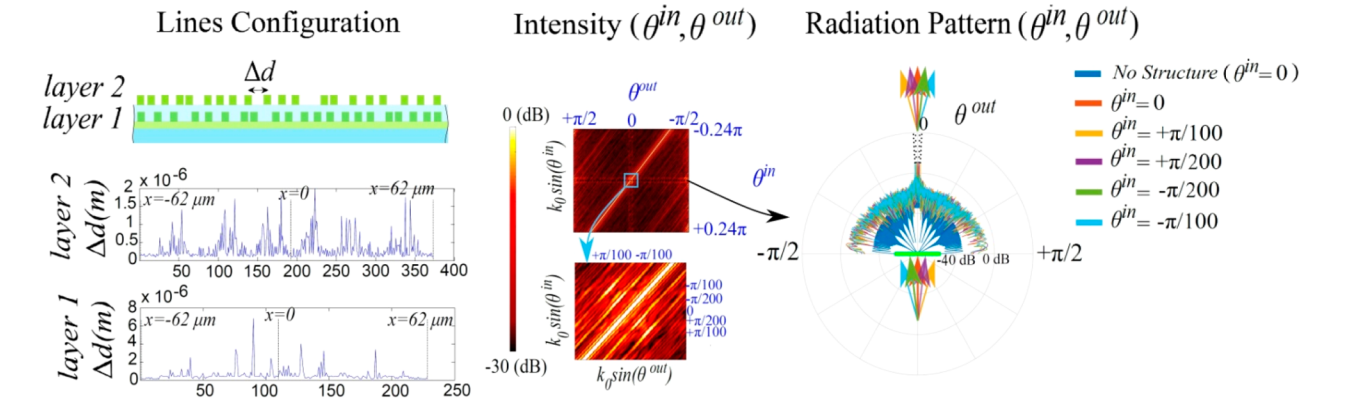

Figure 6. A negative refraction metastructure is realized through engineered disorder. The geometrical size of lines and distance between the layers are the same as those shown in Figure 4. For the preset incident angles, the structure localizes the incident power at corresponding $\theta^{out} = -\theta^{in}$ in the far-field. Like previous designs, high angular sensitivity leads to significant changes in the far-field radiation patterns upon changing the incident angles. The power efficiency for each function is above 10%. The angular characteristics are similar to those of Figure 3a.

angular sensitivity and HPBW remain almost the same as the original structure. Applying random errors to the geometrical sizes of wires (only up to 6% changes in the height or width of lines cross sections), we observe a reduction in efficiency similar to that associated with the errors in locations (up to 30%). A detailed study on the design sensitivity to such errors is provided in the Supporting Information (S4). The results reveal that such designs are fairly tolerant of uncontrollable factors in fabrications leading to errors in the locations of wires, but they bear higher sensitivity with respect to the errors in the geometrical sizes of them.

In the next step, exploiting the available high degrees of freedom, we investigate the capability of such a platform to realize high angular resolution multifunctional metastructures. The problem we address here is the angular multifunctionality, meaning that the structure exhibits various functions for plane waves incident on it at slightly separated angles. Previous works demonstrated how metasurfaces can be designed to interact with preset plane waves to generate different desired images/far-field radiating modes under different angular illuminations.[21,22] The operating principle behind the proposed structures is based on the angular dependence of the scattered fields from the individual scattering elements. This can prevent the incorporation of larger number of functions especially in applications demanding high angular resolutions. Here, we show that our proposed structures can be used to significantly enhance the angular capacity; very small changes in the incident angles are enough to generate a totally different desired output. For this purpose, we demonstrate three different types of designs. In the first type, the metasurfaces perform as far-field concentrators for plane waves illuminating them at angles which are 1.57e-2 radians apart (Figure 5). In a similar manner, in the second type, negative refraction metasurfaces can be designed for a predetermined group of incident plane waves (Figure 6). Moreover, an arbitrary number of functions can be combined and realized in a single design. Shown in Figure 7 is a designed metasurface deflecting the incident plane waves toward preset angular directions depending on their incident angles. The intensity and radiation patterns in Figures 5−7 are normalized with respect to the intensity of the radiated field at ($\theta^{out} = -0.122\pi$, $\theta^{in} = 0$) for the designed structure of Figure 3a. Increasing the number of functions while maintaining the angular sensitivity and HPBW of structures as those shown in Figures 3 and 4, results in the reduction of the efficiency in converting the input incident fields to desired outputs for each plane wave. The efficiency drops to above 10% for the structures shown in Figures 5−7. This can be enhanced by

https://dx.doi.org/10.1021/acsphotonics.9b01655
ACS Photonics 2020, 7, 991−1000

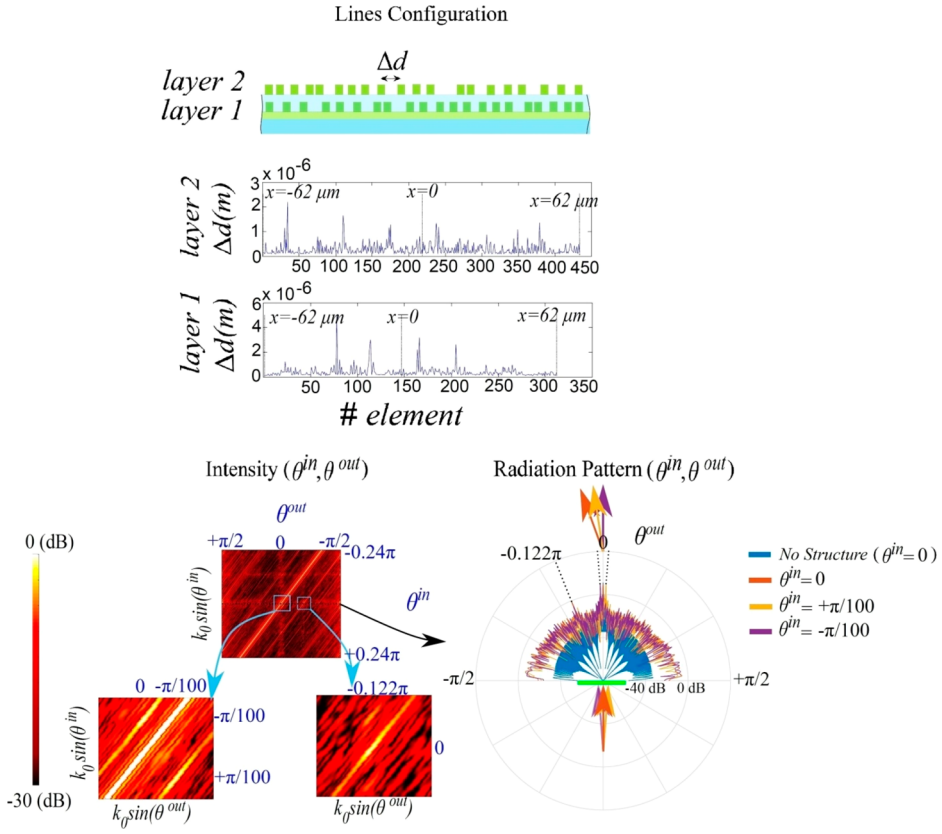

Figure 7. Multifunctional metastructure is realized through engineered disorder. The geometrical size of lines and distance between the layers are the same as those shown in Figures 4–6. For the preset incident angles; $\theta^{in} = 0$, $\pi/100$, and $-\pi/100$, the structure localizes the incident power at $\theta^{out} = -0.122\pi$, $-\pi/100$, and 0, respectively, in the far-field. Like previous designs, high angular sensitivity leads to significant changes in the far-field radiation patterns upon changing the incident angles. The power efficiency for each function is above 10%. The angular characteristics are similar to those of Figure 3a.

adding more layers above structures improving the guided waves coupling mechanism or using thicker multimode dielectric slabs enhancing the conversion efficiency in multifunctional metadevices. The other approach to enhance the efficiency is to decrease the stray diffractions by increasing the deflection angle(s) in new structures. As also shown in the design of Figure 3b, larger deflection angle, along with larger scattering elements, improve the efficiency achieved in the design of Figure 3a. Another important point to highlight is that as we choose to localize the incident fields close to normal output angles ($\theta^{out} \sim 0$), higher angular sensitivities are achieved (Figure 4b and Figure 5). This can be attributed to the longer localization length of associated excited guided waves. Simultaneously, larger accumulations of diffraction orders around $\theta^{out} \sim 0$, which are related to the scattering elements with higher periodicities and their interference with the far-field radiations of the coupled excited guided waves leads to larger $\delta\theta_{in}$ or angular persistency. This effect is favorable in far-field concentrators.

CONCLUSION AND PERSPECTIVE

The implementation of novel functions through metastructures requires the development and application of new strategies in the design and optimization process. Owing to their high degrees of freedom, disordered structures can offer new opportunities to discover novel designs. We investigated disordered metasurfaces with strong short-range (interelement) and long-range (through guided waves) couplings. The disorder induced localization of guided waves play a paramount role in controlling the radiation of such metasurfaces. Being dependent on the initial excitations, the localization of guided waves and their coupling to the far-field radiation are highly sensitive to the incident plane waves angles. Such an effect can be exploited to enhance the angular resolution in multifunctional metasurfaces. Employing a novel inverse design algorithm, highly sensitive angular selectivity, far-field angular concentrators, and negative refraction metasufaces are investigated. Various techniques to enhance the efficiency have been discussed. Although we studied the implementation of the proposed idea for 2D structures, the concept can be straightforwardly applied to 3D cases. The potential applications of disorder engineered structures are far beyond those discussed in this paper. Applications of such versatile designs are highly demanded in emerging optical systems, including LiDARs with multiple beams control, near-field sensors, and highly secure optical/communication systems, to name a few.

ASSOCIATED CONTENT

Supporting Information

The Supporting Information is available free of charge at https://pubs.acs.org/doi/10.1021/acsphotonics.9b01655.

Disorder-induced localization (S1); Guided waves localization (S2); Localization-assisted beamforming (S3); Design sensitivity with respect to the locations

https://dx.doi.org/10.1021/acsphotonics.9b01655
ACS Photonics 2020, 7, 991−1000

and geometrical sizes of scattering elements (S4); Near optimal freeform inverse design (S5) (PDF)

AUTHOR INFORMATION

Corresponding Author

Mohammad Haghtalab − *John A. Paulson School of Engineering and Applied Sciences, Harvard University, Cambridge, Massachusetts 02138, United States; Department of Electrical and Computer Engineering, University of Waterloo, Waterloo, Ontario N2L 3G1, Canada;* orcid.org/0000-0001-6238-1943; Email: mhaghtalab@g.harvard.edu

Authors

Michele Tamagnone − *John A. Paulson School of Engineering and Applied Sciences, Harvard University, Cambridge, Massachusetts 02138, United States;* orcid.org/0000-0002-9812-2449

Alexander Y. Zhu − *John A. Paulson School of Engineering and Applied Sciences, Harvard University, Cambridge, Massachusetts 02138, United States*

Safieddin Safavi-Naeini − *Department of Electrical and Computer Engineering, University of Waterloo, Waterloo, Ontario N2L 3G1, Canada*

Federico Capasso − *John A. Paulson School of Engineering and Applied Sciences, Harvard University, Cambridge, Massachusetts 02138, United States*

Complete contact information is available at: https://pubs.acs.org/10.1021/acsphotonics.9b01655

Notes

The authors declare no competing financial interest.

ACKNOWLEDGMENTS

This work has been supported by the National Science and Engineering Research Council (NSERC) of Canada. M.H. thanks Zhujun Shi, Wei Ting Chen, Yao-Wei Huang, Noah A. Rubin, and Soroush R. Boroujeni for helpful discussions. M.T. acknowledges the support of the Swiss National Science Foundation (SNSF) Grant Nos. 168545 and 177836.

REFERENCES

(1) Capasso, F. The future and promise of flat optics: a personal perspective. *Nanophotonics* **2018**, *7*, 953−957.

(2) Khorasaninejad, M.; Chen, W. T.; Devlin, R. C.; Oh, J.; Zhu, A. Y.; Capasso, F. Metalenses at visible wavelengths: Diffraction-limited focusing and subwavelength resolution imaging. *Science* **2016**, *352*, 1190−1194.

(3) Shi, Z.; Khorasaninejad, M.; Huang, Y. W.; Roques-Carmes, C.; Zhu, A. Y.; Chen, W. T.; Sanjeev, V.; Ding, Z. W.; Tamagnone, M.; Chaudhary, K.; Devlin, R. C.; Qiu, C. W.; Capasso, F. Single-layer metasurface with controllable multiwavelength functions. *Nano Lett.* **2018**, *18*, 2420−2427.

(4) Chen, W. T.; Zhu, A. Y.; Sanjeev, V.; Khorasaninejad, M.; Shi, Z.; Lee, E.; Capasso, F. A broadband achromatic metalens for focusing and imaging in the visible. *Nat. Nanotechnol.* **2018**, *13*, 220−226.

(5) Devlin, R. C.; Ambrosio, A.; Rubin, N. A.; Mueller, J. P. B.; Capasso, F. Arbitrary spin to-orbital angular momentum conversion of light. *Science* **2017**, *358*, 896−901.

(6) Haghtalab, M.; Faraji-Dana, R.; Safavi-Naeini, S. Design and Analysis of Disordered Optical Nanoantenna Structures. *J. Lightwave Technol.* **2016**, *34*, 2838−2847.

(7) Yu, N.; Capasso, F. Flat optics with designer metasurfaces. *Nat. Mater.* **2014**, *13*, 139−150.

(8) Arbabi, A.; Horie, Y.; Ball, A. J.; Bagheri, M.; Faraon, A. Subwavelength-thick lenses with high numerical apertures and large efficiency based on high-contrast transmitarrays. *Nat. Commun.* **2015**, *6*, 7069.

(9) Huang, J.; Encinar, J. A. *Reflectarray Antennas*; Wiley, 2007.

(10) Yang, J.; Sell, D.; Fan, J. A. Freeform metagratings based on complex light scattering dynamics for extreme, high efficiency beam steering. *Ann. Phys.* **2018**, *530*, 1700302.

(11) Lin, Z.; Groever, B.; Capasso, F.; Rodriguez, A. W.; Lončar, M. Topology optimized multi layered metaoptics. *Phys. Rev. Appl.* **2018**, *9*, 044030.

(12) Haghtalab, M.; Safavi-Naeini, S. Freeform engineered disordered metalenses for super- resolution imaging and communication. *Opt. Express* **2018**, *26*, 9749−9771.

(13) Freund, I.; Rosenbluh, M.; Feng, S. Memory effects in propagation of optical waves through disordered media. *Phys. Rev. Lett.* **1988**, *61*, 2328.

(14) Cao, H.; Zhao, Y. G.; Ho, S. T.; Seelig, E. W.; Wang, Q. H.; Chang, R. P. Random laser action in semiconductor powder. *Phys. Rev. Lett.* **1999**, *82*, 2278.

(15) Maguid, E.; Yannai, M.; Faerman, A.; Yulevich, I.; Kleiner, V.; Hasman, E. Disorder-induced optical transition from spin Hall to random Rashba effect. *Science* **2017**, *358*, 1411−1415.

(16) Yu, S.; Piao, X.; Hong, J.; Park, N. Metadisorder for designer light in random systems. *Science Adv.* **2016**, *2*, e1501851.

(17) Qiu, C. W.; Zhang, S.; Capasso, F.; Kivshar, Y. Special Issue on "Ultra-capacity Metasurfaces with Low Dimension and High Efficiency. *ACS Photonics* **2018**, *5*, 1640−1642.

(18) Anderson, P. W. Absence of diffusion in certain random lattices. *Phys. Rev.* **1958**, *109*, 1492−1505.

(19) Martin, L.; Di Giuseppe, G.; Perez-Leija, A.; Keil, R.; Dreisow, F.; Heinrich, M.; Nolte, S.; Szameit, A.; Abouraddy, A. F.; Christodoulides, D. N.; Saleh, B. E. A. Anderson localization in optical waveguide arrays with off-diagonal coupling disorder. *Opt. Express* **2011**, *19*, 13636−13646.

(20) Casati, G.; Molinari, L.; Izrailev, F. Scaling properties of band random matrices. *Phys. Rev. Lett.* **1990**, *64*, 1851.

(21) Kamali, S. M.; Arbabi, E.; Arbabi, A.; Horie, Y.; Faraji-Dana, M.; Faraon, A. Angle-multiplexed metasurfaces: Encoding independent wavefronts in a single metasurface under different illumination angles. *Phys. Rev. X* **2017**, *7*, 041056.

(22) Cheng, J.; Inampudi, S.; Mosallaei, H. Optimization-based dielectric metasurfaces for angle-selective multifunctional beam deflection. *Sci. Rep.* **2017**, *7*, 12228.

(23) Zhu, A. Y.; Chen, W. T.; Zaidi, A.; Huang, Y. W.; Khorasaninejad, M.; Sanjeev, V.; Qiu, C. W.; Capasso, F. Giant intrinsic chiro-optical activity in planar dielectric nanostructures. *Light: Sci. Appl.* **2018**, *7*, 17158.

(24) Shi, Z.; Khorasaninejad, M.; Huang, Y. W.; Roques-Carmes, C.; Zhu, A. Y.; Chen, W. T.; Sanjeev, V.; Ding, Z. W.; Tamagnone, M.; Chaudhary, K.; Devlin, R. C.; Qiu, C. W.; Capasso, F. Single-layer metasurface with controllable multiwavelength functions. *Nano Lett.* **2018**, *18*, 2420−2427.

(25) Harrington, R. F. *Field Computation by Moment Methods*; Wiley-IEEE Press, 1993.

(26) Chow, Y. L.; Yang, J. J.; Fang, D. G.; Howard, G. E. A closed form spatial Green's function for the thick microstrip substrate. *IEEE Trans. Microwave Theory Tech.* **1991**, *39*, 588−592.

(27) Haghtalab, M.; Faraji-Dana, R. Integral equation analysis and optimization of 2D layered nanolithography masks by complex images Green's function technique in TM polarization. *J. Opt. Soc. Am. A* **2012**, *29*, 748−756.

(28) Bendsoe, M. P.; Sigmund, O. *Topology Optimization: Theory, Methods and Applications*; Springer Science & Business Media, 2013.

(29) Yang, J.; Fan, J. A. Topology-optimized metasurfaces: impact of initial geometric layout. *Opt. Lett.* **2017**, *42*, 3161−3164.

(30) Wald, A. Contributions to the theory of statistical estimation and testing hypotheses. *Ann. Math. Stat.* **1939**, *10*, 299−326.